Synthesis of 2′-/3′-O-Acylated Adenine Nucleotide Analogs and Their Interactions in Photophosphorylation

G. Onur *, G. Schäfer **, and H. Strotmann *

* Botanisches Institut (Lehrstuhl II, Biochemische Pflanzenphysiologie) der Universität Düsseldorf, Universitätsstraße 1, D-4000 Düsseldorf

** Institut für Biochemie, Medizinische Hochschule Lübeck, Ratzeburger Allee 160, D-2400 Lübeck, Bundesrepublik Deutschland

Z. Naturforsch. **38 c**, 49–59 (1983); received October 7, 1982

Nucleotide Analogs, Photophosphorylation, Energy Transfer Inhibition

By mono esterification of 3′(2′)-hydroxyl residues of adenine nucleotides with various carboxylic acids a series of nucleotide analogs is available including fluorescent and photoaffinity labels. Their chemical synthesis is described. The equilibrium between 2′ and 3′ esters is determined by NMR spectroscopy, stability of the esters and their tendency of acyl migration is discussed.

The interaction of the ADP derivatives with the chloroplast ATP synthesizing system is investigated. Actually, the analogs are typical energy transfer inhibitors, strongly inhibiting photophosphorylation and concomitant coupled electron transport (c_{i50} values ranging from 0.3 to 85 μM). On the basis of inhibitory activities of analogs bearing varying 3′-(2′)-substituents, structure-activity relationships are discussed.

The inhibitory properties of the employed ADP analogs are based on their specific interaction with the catalytic ADP binding site of CF_1 and their extremely slow phosphorylation on the enzyme (rate 0.25% or less compared to ADP phosphorylation). Inhibition is competitive to ADP but non-competitive with regard to P_i. It is specific for the ADP derivatives, whereas the corresponding ATP analogs are only weak inhibitors in phosphorylation and the AMP derivatives are completely inactive. In light-triggered ATP hydrolysis, however, the ATP analogs exhibit an even stronger competitive inhibition than the ADP derivatives. The results suggest that a conformational change of ATPase takes place when the chloroplasts are transferred from energized to de-energized conditions which greatly affects the properties of the active site with respect to nucleotide binding.

Introduction

A variety of modified adenine nucleotides has been employed in studies on ATP hydrolyzing and ATP synthesizing systems like mitochondria and chloroplasts [1 – 6]. Several chemical alterations, particularly at the ribose moiety, can be achieved without affecting the properties of the resulting nucleotide analog with regard to binding and phosphorylation or hydrolysis, respectively, in chloroplasts and isolated chloroplast-ATPase [7, 8]. Thus 2′- and 3′-methylated or -deoxidized ADP analogs can fully replace the parental nucleotide in photophosphorylation and the corresponding ATP analogs are entire substrates in the reverse reaction. On the other hand, 3′-O-acylated ADP derivatives display high affinities to CF_1, but stongly inhibit photophosphorylation of ADP, due to their effective competition on the active site and due to their extremely slow phosphorylation by the enzyme. These compounds in general are useful tools in enzymatic studies of nucleotide-dependent reactions, since they offer the possibility to investigate the process of nucleotide binding practically unaffected by a subsequent enzymatic conversion. This has been exemplified with isolated F_1-ATPase from beefheart mitochondria revealing a total of three high affinity sites, as well as with submitochondrial vesicles [9, 10]. Other successful applications of these derivatives were reported on the mitochondrial adenine nucleotide carrier demonstrating a unique interaction with only one particular conformation of this membrane protein [11]. Furthermore, based on the same chemical modification, covalently linking photoaffinity labels are available

Abbreviations: AdN, adenine-nucleotide; AMP, ADP, ATP, adenosine, mono-, di-, and triphosphate; DMAN-derivatives, 3′(2′)-O-(5-dimethylaminonaphthoyl-1-)adenine-nucleotides; DMF, dimethylformamide; DMSO, dimethylsulphoxide; FCCP, carbonylcyanide-*p*-trifluoromethoxyphenylhydrazone; N-ADP, 3′(2′)-O-(naphthoyl-1-)ADP; NMR, nuclear magnetic resonance; S, solvent system; TLC, thin-layer chromatography; TMS, tetramethylsilane; TNP-analogs, 2′-3′-O-(2,4,6-trinitrophenyl)-adenine-nucleotides; TRIS, tris-(hydroxymethyl)-aminoethane.

Reprint requests to Dr. G. Onur.

0341-0382/83/0100-0049 $ 01.30/0

[6] which might also permit conclusions on the locations and qualities of catalytic and other (presumably regulatory) nucleotide binding sites. The correlation of catalytic inactivation and stoichiometry of photolabeling of F_1-ATPase has recently been communicated [12].

Because of the great interest in this type of compounds, their chemical synthesis and physiochemical properties are described in the present paper. Moreover some basic biochemical results concerning their interaction in the chloroplast ATP synthesizing system are reported.

Materials and Methods

Chromatography

TLC, including preparative TLC, was performed a) on cellulose plates (Merck, 5716) pretreated with water and dried before being developed in following solvent systems, (v : v):

S_1: *n*-butanol : *iso*-propanol : water; (1 : 1 : 1)
S_2: *n*-butanol : *iso*-propanol : water; (1 : 2 : 1)
S_3: *n*-butanol : dioxane : water; (3 : 3 : 2)
S_4: *n*-butanol : methanol : *iso*-propanol : water; (1 : 1 : 1 : 1)
S_5: *n*-butanol : acetic acid : water (5 : 3 : 2)

b) on DC-Micro-Cards SI E (Riedel de Haen, 37341) or silicagel plates (Merck, 5717), using following solvent systems:

S_6: dichloromethane : methanol; (19 : 1)
S_7: dichloromethane : methanol; (9 : 1)
S_8: toluene : acetic acid; (3 : 1)
S_9: toluene : acetic acid; (9 : 1)
S_{10}: ether : petroleum ether; (3 : 1).

Spectroscopy

^{1}H-NMR spectra were recorded at 270 MHz (Bruker WH 270) operating in the Fourier transform mode and locked on the deuterium of the solvent (D_2O, DMSO-D_6, $CDCl_3$, CD_3OD) using TMS as internal standard. Chemical shifts are expressed in ppm, coupling constants J in Hz (s, singulett; d, doublett; dd, double doublett; q, quartett; m, multiplett). IR spectra were obtained by using a Unicam (SP-1000) instrument; maximal absorption band frequenced are given by the wave number ν which is expressed in cm^{-1}. Mass spectra were recorded on a Kratos (MS-30) mass spectrometer. UV-spectroscopic measurements were made with a Cary (Model 14) spectrophotometer or with a Zeiss (DMR 16). Melting points were determined on an Electrothermal (IA 6304) melting point apparatus and are not corrected.

Biochemical assays

Chloroplasts were isolated from spinach leaves as in [13]. Measurements of electron transport, photophosphorylation and light-triggered ATPase were performed as described elsewhere [14].

Enzymes and chemicals

Alkaline phosphatase (from calf intestine) was purchased from Boehringer Mannheim GmbH. All other chemicals were obtained p.a. from commercial sources.

Procedures for syntheses of the nucleotide analogs

The general procedure is presented in Scheme 1.

The respective carboxylic acid (1.0 mmol) and carbonyldiimidazole (1.1 mmol) were stirred in dry DMF (0.5 ml) for half an hour at room temperature under exclusion of moisture. This mixture was then added to the aqueous nucleotide solution (0.3 mmol for the condensation with aliphatic- and 0.5 mmol with aromatic carboxylic acids, dissolved in water, 2.5 ml).

The reaction mixture was stirred for 4 h at room temperature followed by removal of the solvent at reduced pressure. The residue was treated with small portions of acetone and centrifuged.

The precipitate was separated, dissolved in water, and the aqueous solution was subjected to preparative TLC on cellulose (Solv. system $S_1 - S_5$). After being detected under UV-light, the respective major absorbing bands were scraped off, the substances eluted with water, and the aqueous eluates were

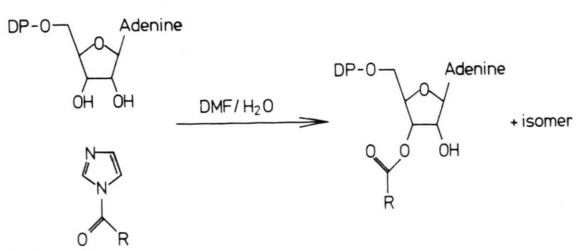

Scheme 1

centrifuged (to remove traces of cellulose) and the supernatants lyophilized. (The yields of the monoesters were 10 – 20% with respect to the nucleotides). The purity of the compounds was checked by TLC in solvent systems $S_1 - S_5$; R_f-values are listed in Table I. Molar extinction coefficients of the analogs are based on respective concentrations determined by phosphate analysis.

3′-O-(naphthoyl-1-)-, and 3′-O-(5-dimethylamino-naphthoyl-1-)adenosine

The respective carboxylic acid (1.0 mmol) and carbonyldiimidazol (1.1 mmol) were dissolved in dry DMF (5 ml) and stirred for half an hour at room temperature under exclusion of moisture. This mixture was then added to the adenosine solution (1.5 mmol in dry DMF (5 ml) containing sodium methylate (0.1 mmol)). The reaction was kept for 24 h at 70 °C, followed by addition of glacial acetic acid (1.0 ml), evaporation of the solvent at vacuum, and treatment of the residual oil with ice-water. The precipitate was separated, washed with small portions of cold water and recrystallized from ethanol-water (3 : 2, v : v). The latter procedure yielded pure 3′-isomers. Further pure 3′-products could be obtained from the mother liquors by preparative TLC on silicagel using solvent system (S_8). In each case, the yields of the 3′-esters were 50 – 60% with respect to the carboxylic acid. The purity of the compounds was checked by TLC (micro cards, solvent system S_8).

3′-O-(naphthoyl-1-)adenosine

m.p., 204 – 205 °C; UV (methanol), $\lambda_{max} = 259$ nm ($\varepsilon = 16700$); IR (KBr), 3360, 3210, 1730, 1655, 1585, 1435, 1250; MS, $m/e = 421$; NMR (DMSO-D_6), 8.86 (1, d, arom., $J = 8.5$), 8.47 (1, s, H_8), 8.34 (1, d, arom., $J = 7.0$), 8.26 (1, d, arom., $J = 8.5$), 8.21 (1, s, H_2), 8.08 (1, d, arom., $J = 7.0$), 7.80 – 7.55 (3, m, arom.), 7.49 (2, s, NH_2, broad, disappeared on addition of D_2O), 6.10 (1, d, 2′-OH, $J = 6.0$, disappeared on addition of D_2O), 6.07 (1, d, H_1', $J_{1',2'} = 7.5$, partially overlapping with 2′-OH), 5.86 (1, dd, 5′-OH, $J = 2.5$, 5.0, disappeared on addition of D_2O), 5.71 (1, dd, H_3', $J_{2',3'} = 5.5$, $J_{3',4'} = 1.8$), 5.14 (1, m, H_2', $J_{1',2'} = 7.5$, $J_{2',3'} = 5.5$), 4.43 (1, d, H_4', $J_{3',4'} = 1.8$), 3.80 (2, m, H_5').

3′-O-(5-dimethylaminonaphthoyl-1-)adenosine

m.p. 179 – 180 °C; UV (methanol), $\lambda_{max} = 256$ nm ($\varepsilon = 27000$); IR (KBr), 3500 – 3000, 2930, 1715, 1645, 1600, 1580; MS, $m/e = 464$, NMR (DMSO-D_6), 8.50 (1, d, arom., $J = 8.5$), 8.43 (1, s, H_8), 8.42 (1, d, arom., partially overlapping with H_8, $J = 8.5$), 8.26 (1, dd, arom., $J = 7.5$, 8.5), 8.18 (1, s, H_2), 7.66 (1, dd, arom., $J = 7.5$, 8.5), 7.58 (1, dd, arom., $J = 7.5$, 8.5), 7.45 (2, s, broad, NH_2, disappeared on addition of D_2O), 7.24 (1, dd, arom., $J = 1.5$, 7.5), 6.06 (1, d, 2′-OH, $J = 6.0$, disappeared on addition of D_2O), 6.03 (1, d, H_1', $J_{1',2'} = 7.0$, partially overlapping with 2′-OH), 5.66 (1, dd, H_3', $J_{2',3'} = 5.5$, $J_{3',4'} = 2.0$), 5.07 (1, m, H_2', $J_{1',2'} = 7.0$, $J_{2',3'} = 5.5$), 4.41 (1, m, H_4', $J_{3',4'} = 2.0$), 3.78 (2, m, H_5'), 2.82 (6, s, $N(CH_3)_2$).

Degradation of nucleotide analogs with alkaline phosphatase

3 – 4 µmol of compounds (10, 11), were incubated with alkaline phosphatase (5 µl, 3 units) in 300 µl TRIS/$MgCl_2$-buffer (0.2 mM/0.5 mM, pH 8.0) at 37 °C. After 5 min a precipitate could be recognized, already. The reaction was maintained for 12 h at this temperature, followed by separation of the precipitate by centrifugation, washing with several small portions of cold water and drying over P_2O_5 under vacuum.

In each case, the isolated products were shown to be pure 3′-isomers by TLC (micro cards, S_7, S_8). The final proof of their structure was followed from their NMR-spectra, which were identical with that of, 3′-O-(naphthoyl-1-)adenosine and 3′-O-(5-dimethylaminonaphthoyl-1-)adenosine, respectively.

Photolabel-carboxylic acids (Scheme 2)

3-(4-amino-2-nitrophenyl)propionic acid (**III**, $n = 2$) was prepared by the method described in [15]. The respective procedure applied to 4-phenylbutyric acid (**I**, $n = 3$) gave 4-(4-amino-2-nitro-

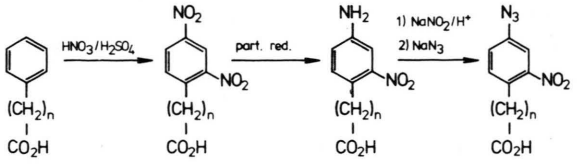

I II III IV

Scheme 2

phenyl)butyric acid (**III**, $n = 3$). Recrystallization of the crude reaction product from water yielded 60% of pure substance; m.p., 127–129 °C (the purity of this compound was checked by TLC, micro cards, solvent system S_6).

UV (methanol), $\lambda_{max} = 270$ nm ($\varepsilon = 14000$); IR (KBr), 3480, 3400, 3300–2500 (broad), 1705, 1640, 1535, 1345; MS, $m/e = 224$; NMR (CD_3OD), 7.18 (1, d, $J = 3.0$), 7.11 (1, d, $J = 9.0$), 6.87 (1, dd, $J = 3.0, 9.0$), 2.73 (2, t, $J = 7.5$), 2.30 (2, t, $J = 7.5$), 1.86 (2, quintett, $J = 7.5$).

Compounds (**III**, $n = 2, 3$) were converted to the corresponding azido-derivatives (**IV**) according [16]. The reaction products were recrystallized from water (yields: 60–70%).

*3-(4-azido-2-nitrophenyl)-propionic acid (**IV**, $n = 2$)*

m.p., 127–128 °C (decomposition); TLC (micro cards, solvent system S_6 or S_{10}); UV (methanol), $\lambda_{max} = 245$ nm ($\varepsilon = 17700$); IR (KBr), 3300–2600 (broad), 2130, 1705, 1535, 1435, 1495, 1330; MS, $m/e = 236$; NMR (DMSO-D_6), 7.63 (1, d, $J = 2.5$), 7.55 (1, d, $J = 8.0$) 7.41 (1, dd, $J = 2.5, 8.0$), 3.02 (2, t, $J = 7.5$), 2.58 (2, t, $J = 7.5$).

*4-(4-azido-2-nitrophenyl)-butyric acid (**IV**, $n = 3$)*

m.p., 106–107 °C (decomposition); TCL (micro cards, S_5 or S_9); UV (methanol), $\lambda_{max} = 245$ nm ($\varepsilon = 18000$); IR (KBr), 3200–2700 (broad), 2150, 1705, 1535, 1495, 1435, 1330; MS, $m/e = 250$; NMR (DMSO-D_6), 7.64 (1, d, $J = 1.8$), 7.54 (1, d, $J = 8,5$), 7.44 (1, dd, $J = 1.8, 8.5$), 2.78 (2, t, $J = 8.0$), 2.25 (2, t, $J = 8.0$), 1.79 (2, quintett, $J = 8.0$).

Fluorescent carboxylic acids

5-dimethylaminonaphthalene-1-carboxylic acid (**VI** Scheme 3) was prepared from 5-aminonaphthalene-1-carboxylic acid (**V**) (for synthesis see [17, 18]) in the following manner: The acid (1.0 mmol) was dissolved in $NaHCO_3$-solution (5 ml, 4 M), which was then transferred into a tube equipped with a magnetic stirrer, After addition of methyliodide (8 mmol) the

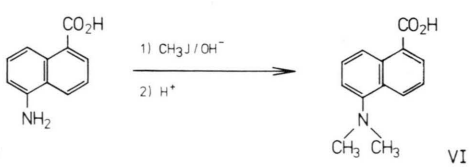

V VI

Scheme 3

tube was sealed, placed in a water bath (70 °C) and stirred for 12 h at this temperature. The alkaline reaction mixture was then acidified (pH 4.0) and the precipitate was extracted with small portions of ethylacetate. Removal of the solvent at reduced pressure followed by recrystallization of the residual oil from petroleumether (45–75 °C) gave pure (**VI**) as fine orange needles (yield: 60%). The purity of this compound was checked by TLC (micro cards, solvent system S_7 or S_9). m.p., 134–135 °C; UV (methanol), $\lambda_{max} = 243$ nm ($\varepsilon = 13500$); IR (KBr), 3200–2500 (broad), 1695, 1580, 1470, 1285; MS, $m/e = 215$; NMR (DMSO-D_6). 8.46 (1, dd, $J = 1.0, 8.5$), 8.42 (1, d, $J = 8.5$), 8.09 (1, dd, $J = 1.0, 7.5$), 7.58 (1, dd, $J = 7.5, 8.5$), 7.53 (1, dd, $J = 7.5, 8.5$), 7.20 (1, d, $J = 7.5$). 2.83 (6, s, $N(CH_3)_2$).

Anthracene-1-carboxylic acid was synthesized from benzene-1-2-3-tricarboxylic acid according to [19, 20].

Results and Discussion

I. Chemical Part

1. Monoacylation of the ribonucleotide cis 2′-3′-diol system

The chemical modification of adenine-nucleotides represents an esterification of an activated carboxylic acid by hydroxyl residues of ribose (Scheme 1).

Carboxyl activation by carbodiimidazole [21], was first applied for the synthesis of amino acid esters of nucleosides and nucleotides [22]. This method was adapted also for substrate modifications, especially in order to prepare analogs, bearing photo-reactive residues [23]. The action of the amino-group attached to the 6-position of the heterocyclic moiety as a competitive nucleophile can be obviated by suitable choice of the reaction medium. Thus, mixtures of water with weakly solvating aprotonic solvents were found to fulfil these requirements [22].

In this work carboxylic acids (aliphatic, araliphatic, aromatic) were chosen as coupling partners, and under the employed conditions (see Methods) the reaction of adenine nucleotides with carboxylic acid imidazolides was found to take place at both, 2′- and 3′-ribose hydroxyls. Dependent on the molar ratio imidazolide/nucleotide, diester formation was also observed; the higher the nucleotide concentration, the lower was the formation of diester.

Table I. Structure of ADP-analogs synthesized according to Scheme 1 and their half-maximal inhibitory concentrations (I_{50}) in photophosphorylation. [+]) UV-spectra were taken in 0.1 M P_i-buffer (pH = 7.0); [++]) Photophosphorylation was measured in a methylviologen system with hexokinase trap as described in Methods (see also Fig. 2 legend). The concentration of the analogs for the assays were estimated by respective molar extinction coefficients or by P_i-analysis.

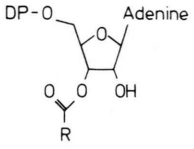

Cp. Nr.	-R	Chromatogr. Solv.	R_f	Absorption[+]) λ_{max} (nm)	ε ($M^{-1}cm^{-1}$)	Inhibition[++]) I_{50} (μM)
1	$-CH_3$	1	0.44	259		85
2	$-C_5H_{11}$	1	0.46	259		20
3	$-CH_2-C(CH_3)_3$	1	0.48	259		22
4	$-C_7H_{15}$	1	0.48	259		41
5	$-CH_2$-Ph	1	0.44	259		9
6	$-(CH_2)_2$-Ph(N_3)(NO_2)	1 2	0.58 0.35	249	27100	20
7	$-(CH_2)_3$-Ph	2	0.40	259		12
8	$-(CH_2)_3$-Ph(N_3)(NO_2)	1 2	0.60 0.40	249	27000	43
9	-Ph	1	0.51	259		26
10	-Naphthyl	1	0.37	259	12000	0.3
11	-Naphthyl($N(CH_3)_2$)	1 3	0.38 0.43	252	13800	0.4
12	-Anthracenyl	1 3	0.55 0.40	254		0.6

Although a clear separation of diester from monoester was possible, a separation of corresponding 2′- and 3′-isomers failed. In each case the monoacyl-derivatives of ADP were isolated as an isomeric mixture, containing both, 2′- and 3′-esters, the latter being the predominant species (70%), as shown below.

Table I shows a list of analogs prepared according to the imidazolide-method. The structures of the nucleotide analogs were ascertained by phosphate-analysis, IR-, UV-, and especially by NMR-spectroscopy. In some cases the analogs were also subjected to degradation by alkaline phosphatase. Precursor carboxylic acids of the analogs which were not available from commercial sources were synthesized separately (compounds **6**, **8**, **11**, **12** in Table I).

2. Identification and distinction of monoacyl-derivatives by NMR-spectroscopy

A clear discrimination between 2′- and 3′-esters can be made by means of the NMR-spectrum of a mixture containing both isomers in comparison with the spectrum of one pure component (2′ or 3′). This makes it necessary to isolate one of the products free from contamination by the other.

It is well known, that monoacyl-derivatives of *cis* 1,2-diol systems easily undergo isomerisation by acyl-migration [24, 25], and the isomerisation rate depends on the nature (mobility) of the acyl-substituent. Aliphatic acyl substituents (*i.e.*, formyl- and acetyl-residues) were found to migrate much more readily than aromatic acyl-substituents (*i.e.*, benzoyl-residue). In this context isolation of one pure isomer, especially an aromatic monoacyl derivative, was necessary, in which the acyl migration rate was low enough for taking a specific NMR-spectrum.

Actually, it was possible to isolate pure 3′-esters of adenosine, bearing condensed aromatic ring systems as 3′-substituents which allowed a differentiation between 2′- and 3′-products.

A useful information for NMR-spectroscopical asignment of isomers is given by the chemical shift of the anomeric proton H_1', which should be at lower field for the 2′ than for the 3′-product; moreover, the coupling constant $J_{1'2'}$ for the 3′-compound should have a higher value than $J_{1'2'}$ for the 2′-compound. This chemical shift rule is based on the electronic influence of the respective substituents [26, 27]: electron-withdrawing groups attached to 2′-OH residue would have a greater deshielding effect on H_1' than in case of 3′-isomers where the electrophilic substituent is more remote from this proton.

Isomeric 2′- and 3′-esters show differences in chemical shifts of H_1'-resonances, varying between 0.25 (aliphatic substituents) and 0.35 ppm (aromatic residues). This fact allowed the determination of 2′/3′-ratios in a mixture by integration of the corresponding H_1'-doubletts. Such an estimation is il-

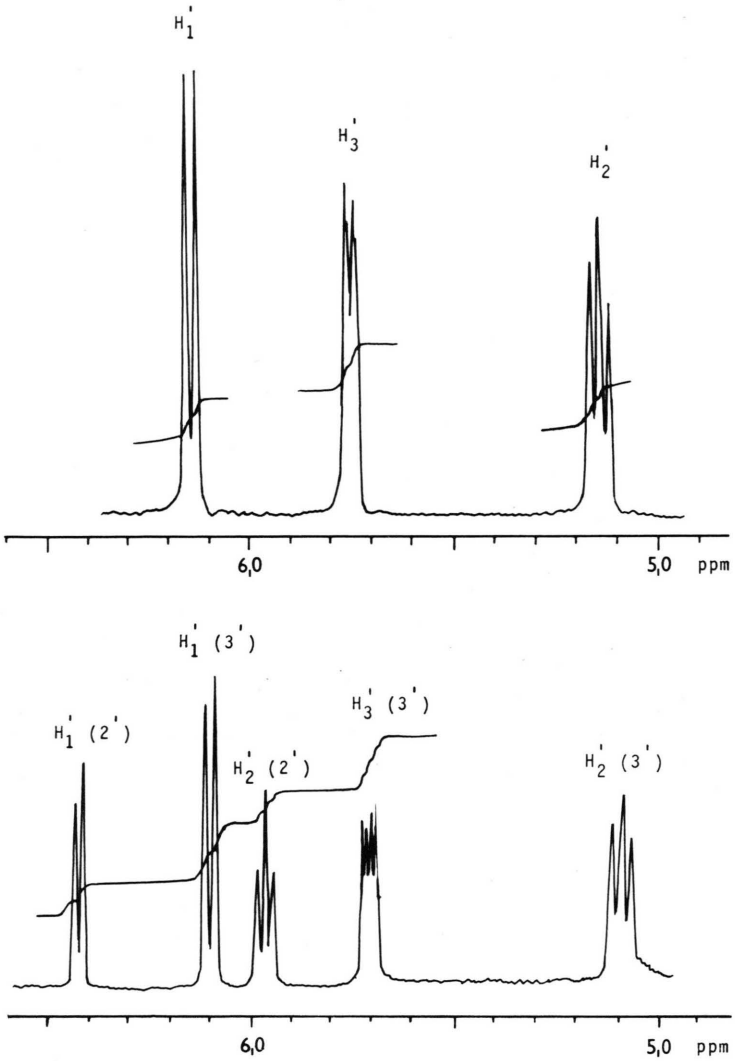

Fig. 1. H_1', H_2', and H_3' resonance signals of 3′-O-naphthoyl-1-adenosine (upper spectrum, 50 scans), and naphthoyl-1-ADP (**10**) (lower spectrum, 100 scans). ^{1}H-NMR spectra were taken in DMSO-D_6/D_2O (8/1, v/v) at 30 °C with a digital resolution of 0.1 Hz. The concentrations were 10, and 5 mM, respectivley. The coupling constant $J_{1',2'}$ of H_1' was 5.5 Hz for 2′-, and 7.5 Hz for 3′-isomer (lower spectrum). The isomeric mixture contained 31% 2′- and 69% 3′-ester, as being estimated by integration of H_1' resonances.

lustrated in Fig. 1, where a ^{1}N-NMR-spectrum of pure 3′-O-(naphthoyl-1-)-adenosine is compared with the spectrum of an isomeric mixture containing 2′- and 3′-O-(naphthoyl-1)-ADP (**10**). As this example shows, the resonance signals of H_2' (2′-isomer) and H_3' (3′-isomer) are also resolved sufficiently enough to be useful to estimate the composition of the isomeric mixture. With all nucleotide analogs investigated so far, this method led to nearly equal 2′/3′-ratios: 3′-isomers revealed to be the predominant species (about 70%) compared to 2′-isomers (about 30%).

3. Enzymatic cleavage of 2′-3′-monoesters mixtures

Enzymatic cleavage of the monoesters of ADP (**10**, **11**) by alkaline-phosphatase in Tris/$MgCl_2$-buffer (pH 8.0, 37 °C) in each case led to a product which precipitated from aqueous solution. These precipitates were shown by NMR-spectroscopy to consist of more than 95% 3′-O-(naphthoyl-1-)adenosine and 3′-O-(5-dimethylaminonaphthoyl-1-)adenosine, respectively.

Examination of the remaining aqueous reaction solution by TLC showed that each of them contained a mixture of 2′- and 3′-isomers.

II. Biochemical part

1. 3'(2')-O-acylated ADP analogs as inhibitors of photophosphorylation

All of the synthesized 3'(2')-O-acylated ADP analogs are more or less strong inhibitors of ADP phosphorylation, depending on the nature of the substituent. This is due to effective competition with the parental nucleotide on one hand, but extremely slow phosphorylation on the other. Thus, the rate of photophosphorylation of N-ADP (**10**) was *e.g.* only 0.15 μmol/mg chl h at 5 μM, that is 400 times less than ADP phosphorylation at the same concentration. The C_{i50} values for inhibition of phosphorylation in a non-cyclic electron transport system with methylviologen as acceptor are listed in Table I.

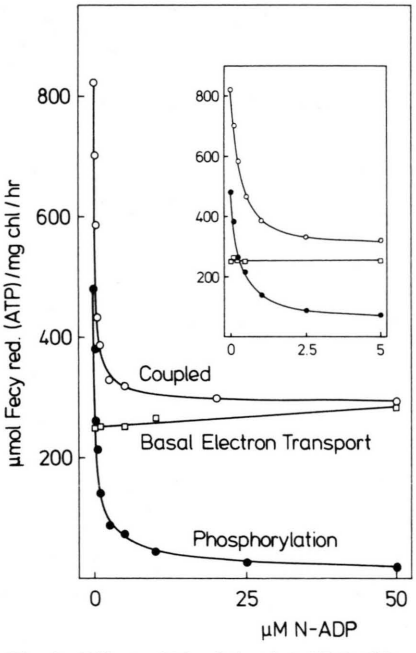

Fig. 2. Effect of Naphthoyl-1-ADP (**10**) on photophosphorylation, coupled and basal electron transport. The incubation medium contained 25 mM tricine buffer (pH 8.0), 50 mM NaCl, 5 mM $MgCl_2$, 0.1 mM ADP and 1 mM K_3 [$Fe(CN)_6$]. Measurements of coupled electron transport and photophosphorylation were carried out in presence of additional 5 mM ^{32}P-P_i, 10 mM glucose and 17.9 units/ml ammonium sulfate-free hexokinase. The reactions were performed at 20 °C in a glass cuvette, using red actinic light (RG 630 filter Schott, intensity 800 W/m^2), incubation volume and chlorophyll content beeing 2.0 ml and 5 μg/ml, respectively. Ferricyanid reduction was registrated by a Zeiss PMQ II spectrophotometer. For photophosphorylation measurements, probes were illuminated for 2 min followed by denaturation by $HClO_4$ (final conc. 0.3 M).

Table II. Effect of N-ADP (**10**) on uncoupled electron transport. Uncoupled chloroplasts were prepared by removal of CF_1 according to the method described in [34]. Methylviologen reduction was measured as outlined in Fig. 3 legend.

Addition	(μ mol O_2/mg Chl h)
None	244.7
None	255.8
None	233.5
N-ADP (10 μM)	222.4
N-ADP (30 μM)	222.4
N-ADP (100 μM)	233.5

Analogs carrying a short chain alkyl group (*e.g.* compound **1**) cause only weak inhibition. The inhibitory activity increases with increasing the chain length (**2**) and also if branched alkyl residues are introduced (**3**). Further elongation of the aliphatic chain (**4**) again decreases the inhibitory effect.

Introduction of aromatic residues as substituents in alkyl chains of varying length yields inhibitors of intermediate effectiveness (**5**–**9**). A dramatic increase in the inhibitory power is, however, attained, if condensed aromatic rings without a spacing alkyl chain are introduced. Thus, the most potent inhibitors of photophosphorylation are the naphthoyl- and anthranoyl-derivatives of ADP (**10**–**12**). Most of the subsequently described experiments have therefore been performed with these compounds.

2. Action as energy transfer inhibitors

In Fig. 2 the effect of N-ADP (**10**) on basal and coupled electron transport as well as on the rate of phosphorylation is shown. The results reveal the typical characteristics of energy transfer inhibition of coupled electron transport concomitant to inhibition of ATP synthesis ($C_{i50} = 0.5$ μM) while basal electron flow is unaffected. Moreover, Table II demonstrates that uncoupled electron transport is also completely unaffected and Fig. 3 shows that inhibition of coupled electron transport is released by addition of an uncoupler. Hence N-ADP is a pure and one of the most effective energy transfer inhibitors in photophosphorylation.

Fig. 4 compares the effects of DMAN-derivatives of AMP, ADP (**11**) and ATP on photophosphorylation. The results clearly demonstrate that powerful inhibition of ATP synthesis is obtained by the ADP

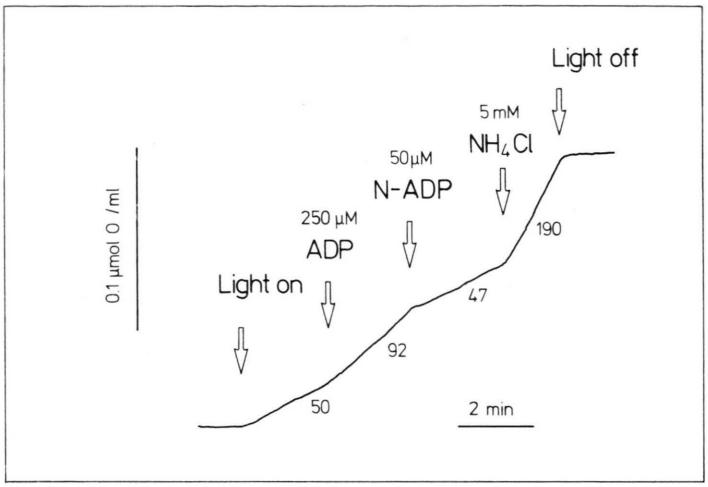

Fig. 3. Inhibition of coupled electron transport by N-ADP (**10**) and release of inhibition by uncoupling. The medium contained the components as detailed in Fig. 2 legend except that ferricyanide was replaced by 0.5 mM methylviologen. 1 mm KCN was added. Oxygen uptake was measured using a Clark type electrode. The reaction was performed at 20 °C, light-intensity was 350 W/m^2 (red light, Filter RG 630, Schott).

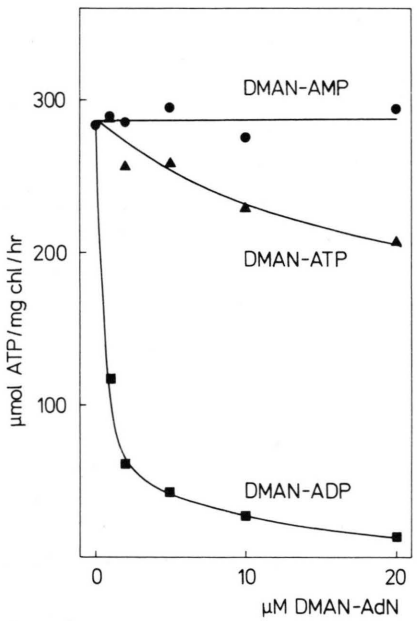

Fig. 4. Effect of 5-dimethylaminonaphthoyl-1-derivatives of AMP, ADP (**11**) and ATP on photophosphorylation. For experimental details see Fig. 2 legend.

analog only ($C_{i50} = 1$ µM), the ATP analog being much less effective ($C_{i50} = 20$ µM) while the AMP derivative is completely inactive, a result which exactly resembles the action on oxidative phosphorylation [28].

3. Inhibiton kinetics

The effects of N-ADP on steady state kinetics of photophosphorylation are investigated in Figs. 5 and 6. In an experiment shown in Fig. 5, phosphate concentration was varied in the absence and presence of 2.5 µM N-ADP. The substrate ADP was present at 20 µM or 200 µM, respectively. With regard to phosphate, N-ADP acts as a noncompetitive inhibitor, the inhibitory effect being more pronounced at low compared to high concentration of ADP. Phosphorylation as a function of ADP in the absence and presence of N-ADP and N-ATP, respectively, is shown in Fig. 7. Moreover two different light intensities were employed. V_{max} as well as apparent K_m have been reported to depend on the efficiency of electron transport and can therefore be modulated by the employed light intensity. At varying light both parameters are linearly related to each other [29]. Both, N-ADP and N-ATP act as competitive inhibitors with respect to ADP. While the K_i values for the ATP analog are almost independent of the light intensity, a more effective inhibition by the ADP analog is obtained at low light compared to light saturation. In some experiments (Fig. 6, Fig. 7, top) a deflection from linearity in the double-reciprocal plot was observed at low ADP concentrations in presence of N-ADP, indicating sigmoidal kinetics. A similar observation has been made in oxidative phosphorylation of submitochondrial particles and interpreted as an indication of cooperativity of at least two interdependent catalytic nucleotide binding sites [30].

The competitive effect of the ATP analog is low compared to the ADP analog. The apparent K_i values differ by a factor of 20 (high light) or even more at low light intensity (Fig. 7). For oxidative

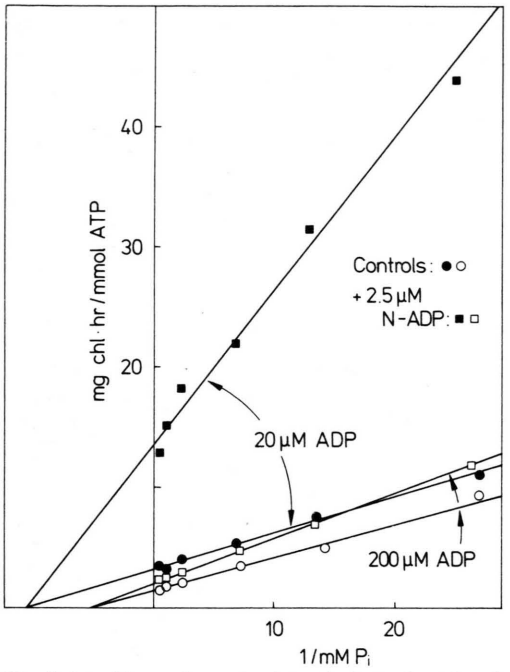

Fig. 5. Double reciprocal plot of photophosphorylation of ADP: dependence on phosphate concentration in the presence and absence of naphthoyl-1-ADP (**10**) as inhibitor. For experimental conditions see Fig. 2 legend.

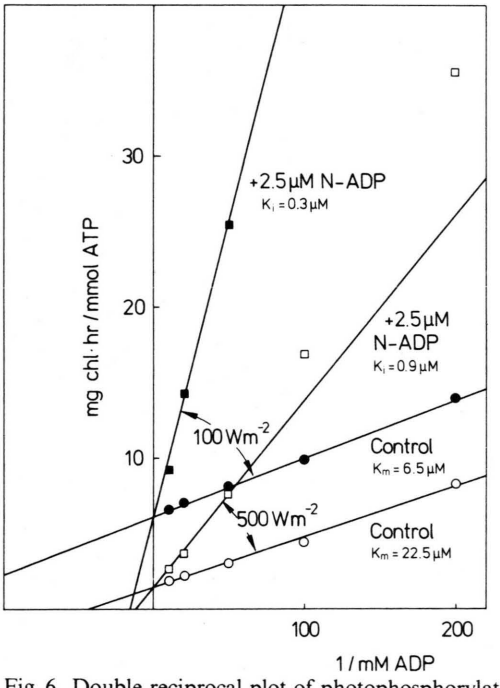

Fig. 6. Double reciprocal plot of photophosphorylation with ADP as variable substrate in the presence and absence of N-ADP (**10**) at two different light intensities. Experimental conditions in this assay were equal to that outlined in Fig. 2 legend.

phosphorylation in submitochondrial particles factors of more than 100 have been observed [31].

From the fact that both analogs are competitive inhibitors with respect to ADP, their K_i-values reflect affinities to the catalytic ADP binding site under phosphorylating conditions. Moreover the conclusion is also permitted that they indicate the relative affinities of the parental compounds ADP and ATP, respectively. Accordingly, in phosphorylating chloroplasts, ATPase exhibits a high selectivity for ADP compared to ATP [14].

In the reverse reaction (light-triggered ATP hydrolysis) both analogs are competitive inhibitors

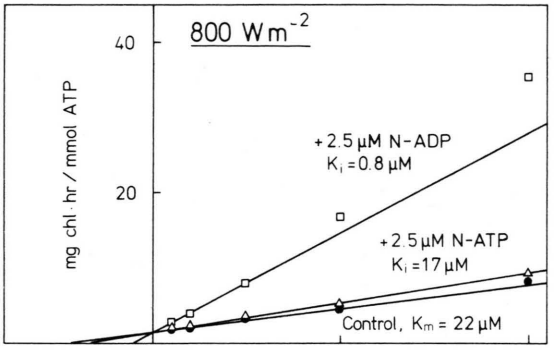

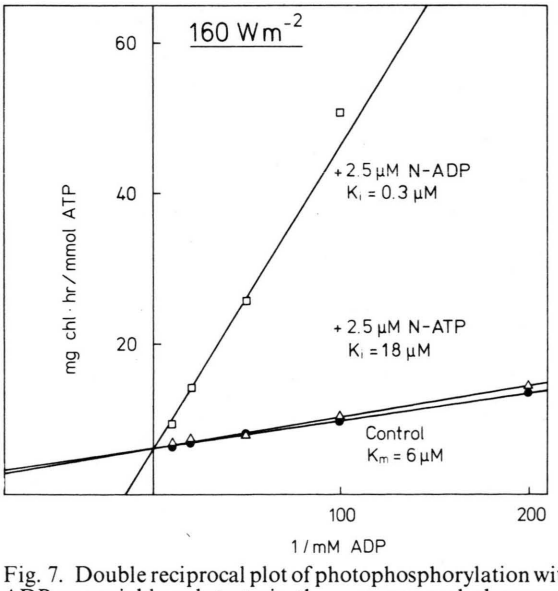

Fig. 7. Double reciprocal plot of photophosphorylation with ADP as variable substrate in the presence and absence of naphthoyl-1-derivatives of ADP (**10**) and ATP, respectively, at two different light intensities. For experimental details see Fig. 2 legend.

Table III. Effects of N-ADP (**10**) and N-ATP on ATP formation and ATP hydrolysis represented in terms of K_i-values. K_m values determined from the corresponding control experiments were 65 and 83 μM, respectively. For experimental details see [14].

AdN-analog	K_i [μM]	
	ATP-synthesis	ATP-hydrolysis
N-ADP	2.7	5.5
N-ATP	27.0	2.7

likewise [14]. Table III summarizes results of an experiment where ATP synthesis and subsequent dark ADP hydrolysis were studied in the same assay. Limited amounts of ADP were first phosphorylated in the light. Phosphorylation rates were evaluated from the initial increase in ATP. When the light was turned off after reaching the final steady state, the newly synthesized ATP was partially hydrolyzed [14]. The initial rates were evaluated and taken as measures of ATP hydrolyzing activity. In order to measure the effects of N-ADP and -ATP on phosphorylation and ATP hydrolysis, the analogs were added before onset of illumination or at the light-to-dark transition, respectively. Table III confirms the general phenomenon shown in Fig. 7, *i.e.* low K_i for the ADP analog compared to the ATP analog in photophosphorylation. The higher K_i values for both analogs as compared to the experiments of Figs. 5–7 may be due to the change in experimental conditions (absence of a regenerating hexokinase system).

The difference in the apparent K_i-values of both analogs disappears under ATP-hydrolyzing conditions. Even a small increase of the K_i for the ADP-analog over the K_i-value of the ATP-analog can be recognized. Since the only relevant change concerns the state of membrane energization, a conformational transition of ATPase is likely when $\Delta\tilde{\mu}_{H^+}$ is relaxing. This has also been concluded from other types of experiments [32]. Apparently, the assumed conformational change has direct consequence on the properties of the catalytic site.

A recent study on oxidative phosphorylation [31, 33] is in support of this conclusion. Using the same type of analogs and comparing their effects with those of 2′, 3′-TNP-analogs, mitochondrial F_1-ATPase has also been proposed to be a "dual-state"-enzyme, changing its conformation and its ligand interactions depending on the presence of a $\Delta\tilde{\mu}_{H^+}$ across the membrane.

Acknowledgements

This work was supported by grants of the Deutsche Forschungsgemeinschaft. The authors are indebted to Mrs. M. Möller, Mrs. K. Brendel and to Mr. K. Edelmann for excellent technical assistance.

[1] D. A. Hilborn and G. G. Hammes, Biochemistry **12,** 983–990 (1973).
[2] H. A. Lardy, S. M. Schuster, and R. E. Ebel J. Supramol. Struct. **3,** 214–221 (1975).
[3] P. L. Pedersen, J. Supramol. Struct. **3,** 222–230 (1975).
[4] D. A. Harris, J. C. Gomez-Fernandez, L. Klungsøyr, and G. K. Radda, in: Structure and Function of Energy Transducing Membranes (K. van Dam and B. F. van Gelder, eds.) pp. 319–327, Elsevier, Amsterdam 1977.
[5] H. Strotmann, S. Bickel-Sandkötter, K. Edelmann, E. Schlimme, K. S. Boos, and J. Lüstorff, in: Structure and Function of Energy Transducing Membranes (K. van Dam and B. F. van Gelder, eds.), pp. 307–317, Elsevier, Amsterdam 1977.
[6] G. Schäfer and G. Onur, Eur. J. Biochem. **97,** 415–424 (1979).
[7] G. Schäfer, G. Onur, K. Edelmann, S. Bickel-Sandkötter, and H. Strotmann, FEBS Lett. **87,** 318–322 (1978).
[8] U. S. Boos, B. Dimke, E. Schlimme, H. Wiedner, K. Edelmann, and H. Strotmann, FEBS Lett. **130,** 73–76 (1981).
[9] H. Tiedge, U. Lücken, J. Weber, and G. Schäfer, E. J. Biochem., in the press – and: EBEC-Reports **2,** 111–112 (1982); LBTM-CNSR Edition.
[10] G. Schäfer and J. Weber, J. Bioenerg., Biomembranes (special issue), in the press.
[11] G. Schäfer and G. Onur, FEBS Lett. **109,** 197–201 (1980).
[12] J. Weber, U. Lücken, H. Tiedge, G. Onur, and G. Schäfer, EBEC-Reports **2,** 63–64 (1982); LBTM-CNRS Edition.
[13] H. Strotmann and S. Bickel-Sandkötter, Biochim. Biophys. Acta **460,** 126–135 (1977).
[14] U. Franek and H. Strotmann, FEBS Lett. **126,** 5–8 (1981).
[15] S. Gabriel and J. Zimmermann, Ber. Dtsch. Chem. Ges. **13,** 1680 (1880).
[16] G. W. Fleed, J. R. Knowles, and R. Porter, Biochem. J. **128,** 499–508 (1972).
[17] A. G. Ekstrand, J. Prakt. Chem. (2) **38,** 156–244 (1888).
[18] F. Bell and W. H. D. Morgan, J. Chem. Soc., **1954,** 1716–1718.
[19] C. Graebe and M. Leonhardt, Ann. Chem. **290,** 221 (1896).

[20] C. Graebe and S. Blumenfeld, Ber. Dtsch. Chem. Ges. **30,** 1115 (1897).
[21] H. A. Staab and A. Mannschreck, Chem. Ber. **95,** 1284–1297 (1962).
[22] B. P. Gottikh, A. A. Krayevsky, N. B. Tarussova, P. D. Purygin, and T. L. Tsilevich, Tetrahedron **26,** 4419–4433 (1970).
[23] S. J. Jeng and R. J. Guillory, J. Supramol. Struct. **3,** 448–468 (1975).
[24] C. B. Reese and D. R. Trentham, Tetrahedron Letters **29,** 2467–2472 (1965).
[25] C. S. McLaughlin and V. M. Ingram, Biochemistry **4,** 1442–1447 (1965).
[26] H. P. M. Fromageot, B. E. Griffin, C. B. Reese, J. E. Sulston, and D. R. Trentham, Tetrahedron **22,** 705–710 (1966).
[27] B. E. Griffin, M. Jarman, C. B. Reese, J. E. Sulston, and D. R. Trentham, Biochemistry **5,** 3638–3649 (1966).
[28] G. Schäfer, G. Onur, and M. Schlegel, J. Bioenerg. and Biomembranes, **12,** 213–232 (1980).
[29] S. Bickel-Sandkötter and H. Strotmann, FEBS Lett. **125,** 188–192 (1981).
[30] G. Schäfer and G. Onur, FEBS Lett. **117,** 269–272 (1980).
[31] G. Schäfer, FEBS-Letters **139,** 271–275 (1982).
[32] J. Schumann and H. Strotmann, in: Photosynthesis II, Electron Transport and Photophosphorylation (G. Akoyunoglou, ed.), pp. 881–892, Balaban Int. Sci. Serv. Philadelphia, Pa., 1982.
[33] G. Schäfer, EBEC-Reports **2,** 21–22 (1982); LBTM-CNRS Edition.
[34] W. Tischer and H. Strotmann, Biochem. Biophys. Acta **460,** 113–125 (1977).